



UDC 621.762.34

<https://doi.org/10.17073/1997-308X-2024-4-45-54>Research article  
Научная статья

# Dispersion strengthening of powder high-speed steel R6M5K5 with particles of SHS ceramics $\text{MoSi}_2\text{--MoB--HfB}_2$

A. S. Akhmetov<sup>✉</sup>, S. K. Mukanov, M. E. Samoshina,  
V. Yu. Lopatin, Zh. V. Ereemeeva

National University of Science and Technology “MISIS”  
4 bld. 1 Leninskiy Prosp., Moscow 119049, Russia

✉ [aman1aotero@gmail.com](mailto:aman1aotero@gmail.com)

**Abstract.** The possibility of dispersion strengthening of powder high-speed steel R6M5K5 with  $\text{MoSi}_2\text{--MoB--HfB}_2$  heterophase ceramics particles was investigated. A mechanically alloyed powder mixture with an average particle size of  $d = 10 \mu\text{m}$  was used as the base material; the ceramic powder additive ( $d = 5 \mu\text{m}$ ), obtained by the SHS method, was also used. Mixing was carried out in a high planetary ball mill. As a result, powder mixture particles with sizes of 2–25  $\mu\text{m}$  were obtained, close to spherical in shape, with larger particles being agglomerates. Cold pressing and sintering were performed, achieving a density of up to 92.7 % and a hardness of 62 HRA, as well as hot pressing with a density of 97.2 % and a hardness of 65 HRC. The hot-pressed billet had a bending strength of 1141 MPa and a compressive strength of 2157 MPa. The prospects of using heterophase ceramics as a strengthening additive was shown, which contributes to lowering the temperature of the liquid phase formation and creates a pronounced heterogeneous microstructure, similar to the microstructure of metallic glass materials. The matrix is a solid solution based on iron (with an average grain size of 14–34  $\mu\text{m}$ ) with a network of eutectic carbide  $\text{Me}_6\text{C}$  and ceramic additive inclusions in the form of  $\text{HfO}_2$ ,  $\text{SiO}_2$ , and  $\text{HfSiO}_4$  compounds. This provided a twofold reduction in wear during tribological tests against a counterbody made of VK6 hard alloy. The obtained composite material, demonstrating high red hardness, may find application in the production of wear-resistant products operating at temperatures up to 630 °C.

**Keywords:** high-speed steel, powder metallurgy, dispersion hardening, ceramics, tribology, wear

**Acknowledgements:** The research was supported by the Russian Science Foundation grant No. 23-49-00141, <https://rscf.ru/project/23-49-00141/>

**For citation:** Akhmetov A.S., Mukanov S.K., Samoshina M.E., Lopatin V.Yu., Ereemeeva Zh.V. Dispersion strengthening of powder high-speed steel R6M5K5 with particles of SHS ceramics  $\text{MoSi}_2\text{--MoB--HfB}_2$ . *Powder Metallurgy and Functional Coatings*. 2024;18(4):45–54. <https://doi.org/10.17073/1997-308X-2024-4-45-54>

# Дисперсное упрочнение порошковой быстрорежущей стали Р6М5К5 частицами СВС-керамики $\text{MoSi}_2\text{--MoB--HfB}_2$

А. С. Ахметов<sup>✉</sup>, С. К. Муканов, М. Е. Самошина,  
В. Ю. Лопатин, Ж. В. Еремеева

Национальный исследовательский технологический университет «МИСИС»  
Россия, 119049, г. Москва, Ленинский пр-т, 4, стр. 1

✉ aman1aotero@gmail.com

**Аннотация.** Исследована возможность дисперсного упрочнения порошковой быстрорежущей стали Р6М5К5 частицами гетерофазной керамики  $\text{MoSi}_2\text{--MoB--HfB}_2$ . В качестве исходного материала использованы: механически легированная порошковая смесь со средним размером частиц  $d = 10$  мкм; измельченная порошковая керамическая добавка ( $d = 5$  мкм), полученная методом самораспространяющегося высокотемпературного синтеза (СВС). Смешивание осуществлялось в планетарной центробежной мельнице. В результате получены частицы порошковой смеси размером 2–25 мкм, по форме, близкой к округлой, более крупные частицы представляли собой агломераты. Проведены холодное прессование и спекание с достижением плотности до 92,7 % и твердости 62 HRA, а также горячее прессование с плотностью заготовки 97,2 % и твердостью 65 HRC. Горячепрессованная заготовка имела прочность на изгиб 1141 МПа и на сжатие 2157 МПа. Показана перспективность применения гетерофазной керамики в качестве упрочняющей добавки, которая способствует снижению температуры образования жидкой фазы и образует ярко выраженную гетерогенную микроструктуру, схожую с микроструктурой металлокерамических материалов. Матрица – твердый раствор на основе железа (со средним размером зерен 14–34 мкм) с сеткой из эвтектического карбида  $\text{Me}_6\text{C}$  и включениями керамической добавки в виде соединений  $\text{HfO}_2$ ,  $\text{SiO}_2$  и  $\text{HfSiO}_4$ . Это обеспечило уменьшение в 2 раза приведенного износа при трибологических испытаниях в паре с контртелом из твердого сплава ВК6. Полученный композиционный материал, продемонстрировавший высокую красностойкость, может найти применение в изготовлении износостойких изделий, эксплуатируемых при температурах до 630 °С.

**Ключевые слова:** быстрорежущая сталь, порошковая металлургия, дисперсное упрочнение, керамика, трибология, износ

**Благодарности:** Исследование выполнено за счет гранта Российского научного фонда № 23-49-00141, <https://rscf.ru/project/23-49-00141/>

**Для цитирования:** Ахметов А.С., Муканов С.К., Самошина М.Е., Лопатин В.Ю., Еремеева Ж.В. Дисперсное упрочнение порошковой быстрорежущей стали Р6М5К5 частицами СВС-керамики  $\text{MoSi}_2\text{--MoB--HfB}_2$ . *Известия вузов. Порошковая металлургия и функциональные покрытия*. 2024;18(4):45–54. <https://doi.org/10.17073/1997-308X-2024-4-45-54>

## Introduction

Effective combinations of type and content of additives for strengthening powder high-speed steel (HSS) by introducing dispersed hard particles have been widely studied. Generally [1], when selecting strengthening additives, important criteria include their stability at the operating temperatures of the material being strengthened and minimal solubility in the matrix. Carbides such as NbC, TiC, VC, etc. [2–7], and nitrides like VN [8], meet these requirements for HSS. However, compounds that actively interact with the matrix can also be used as dispersed additives. For example, studies [9; 10] investigated the effect of adding boron carbide ( $\text{B}_4\text{C}$ ) on the properties of M3/2 powder steel (analogous to 10R6M5), consolidated by hot pressing. It was found that dispersion strengthening led to an increase in hardness up to 85 HRA, with  $\text{B}_4\text{C}$  particles interacting with the matrix. At optimal concentrations, such an additive can ensure high density at rela-

tively low sintering temperatures ( $t = 1150\div 1190$  °С) due to the interaction of both boron and carbon with the matrix. As a result, these characteristics significantly enhance the physical and mechanical properties of the material [10].

The consolidation of powder high-speed steel with strengthening additives is often performed by pressing and supersolidus sintering or hot pressing (HP), without resorting to hot isostatic pressing [2–11].

Another important aspect in the dispersion strengthening of powder HSS, in addition to the choice of additive and its content, is the method of mixing. Incorrect selection of the method and conditions can lead to particle segregation [12]. Usually, for mixing metal powders with dispersed additives, a planetary ball mill is used, which ensures not only high-quality mixing and uniform distribution of strengthening dispersed particles throughout the charge but also additional grinding of both the strengthening and base

powder particles [13]. As a result, with a proper selection of the mixing mode in the planetary ball mill, a fine-grained structure of the material can be obtained, enhancing its physical and mechanical properties. High dispersion of the powder mixture particles can lead to activated sintering [14]. This also allows for maintaining a fine-grained structure by achieving high density with shorter sintering times, preventing grain growth due to prolonged holding.

The heterophase ceramic  $\text{MoSi}_2\text{--MoB--HfB}_2$ , produced using self-propagating high-temperature synthesis (SHS), is of interest as a strengthening additive due to its high hardness (19.5 GPa) and heat resistance, particularly its resistance to oxidation at elevated temperatures across a wide range [15; 16]. The boron in the ceramic composition can help form a liquid phase at relatively low temperatures and activate the sintering process [10; 17].

Such complex compounds are rarely used as strengthening additives, making the study of their effect on the physical and mechanical properties and microstructure of HSS a pertinent task.

The aim of this work was to produce consolidated samples from a powder mixture of high-speed steel with the addition of heterophase ceramic  $\text{MoSi}_2\text{--MoB--HfB}_2$  and to study their properties to identify promising areas of application for this material.

## Materials and methods

The mechanically alloyed powder mixture of HSS grade R6M5K5 was used as the base material, with the following composition by mass percentage:

W .....	6.0
Mo .....	5.0
Co .....	5.0
Cr .....	4.0
V .....	2.0
C .....	0.9
Fe .....	Rest.

This mixture was obtained by milling in a Planetary ball mill “Activator – 4M” (Russia) at a drum rotation speed of 800 rpm, with a ball-to-powder ratio of 10:1 and a milling time of 30 min. The characteristics of the initial powder components used to produce this mixture are presented in Table 1.

The size range of the main fraction of the mechanically alloyed powder mixture was 3–20  $\mu\text{m}$ , with an average particle diameter of 10  $\mu\text{m}$  and  $D_{50} = 9 \mu\text{m}$ . The mixture consists of solid solutions based on Fe, W, and Mo, as well as WC carbide. The ceramic powder additive had a composition

of 60 % (90 %  $\text{MoSi}_2\text{--}10 \text{ % MoB}$ ) + 40 %  $\text{HfB}_2$ , with an average particle size of 5  $\mu\text{m}$ . The method of its production is described in [15].

The powder steel was mixed with 3 vol. % of the strengthening additive and processed in the Planetary ball mill “Activator – 4M” at a drum rotation speed of 800 rpm, a ball-to-powder ratio of 10:1, and processing times of 15, 30, and 45 min.

The microstructure of the samples was examined using a scanning electron microscope (SEM) S-3400N (Hitachi, Japan) equipped with an energy-dispersive X-ray spectrometer (EDS) NORAN System 7 X-ray Microanalysis System (Thermo Scientific, USA).

X-ray diffraction phase analysis (XRD) of the samples was performed on a D2 PHASER diffractometer (Bruker AXS GmbH, Germany) using  $\text{CuK}_\alpha$  radiation (1.5418 Å).

Particle size distribution was assessed using an ANALYSETTE 22 MicroTec plus (Fritsch GmbH, Germany). The flowability and bulk density of the powder mixture were determined according to GOST 20899-98 and GOST 19440-94, respectively. Additionally, the compressibility during cold pressing and the change in density after sintering were investigated.

Cold pressing of the obtained mixture with and without the ceramic additive was carried out in a steel mold with an inner diameter of 12 mm at pressures ranging from 200 to 900 MPa, and the sintering of the billets was conducted at 1200 °C for 60 min. Hot pressing was performed in a graphite mold with an inner diameter of 20 mm in a Direct Hot Pressing DSP-515 SA press (Dr. Fritsch Sondermaschinen GmbH, Germany) under vacuum at 1000 °C and 50 MPa. The heating and cooling rates were 50 °C/min, with an isothermal holding time of 3 min. The mass of the charge during pressing was calculated to ensure that the height of the pore-free

**Table 1. Characteristics of the initial powder components**

**Таблица 1. Характеристики исходных порошковых компонентов**

Powder grade	Element	GOST/TU	Purity, %
PZhRV 2.200.26	Fe	TU 14-5365-98	99.24
PVCh	W	TU 48-19-57-91	99.99
PM	Mo	TU 14-22-160-2002	99.90
PK	Co	GOST 9721-79	99.95
ERKh-1	Cr	GOST 5905-2004	99.99
FVd50U0,5	V	GOST 27130-94	99.00
P-803	C	GOST 7885-86	99.90

billets was 0.5 times the diameter. Heat treatment (HT) of the obtained hot-pressed billets was carried out under the following conditions: annealing at 800 °C, quenching in oil from 1210 °C, and double tempering at 560 °C [18].

The compressive and flexural strength were evaluated using an LF-100KN testing machine (Walter + Bai, Switzerland). Hardness after hot pressing, heat treatment, and annealing at 630 °C for 4 h (red hardness) was measured using a TR5006 hardness tester (Tochpribor, Russia).

Comparative tribological tests were conducted at room temperature using a Tribometer friction machine (CSM Instruments, Switzerland) in accordance with ASTM G 99-17 and DIN 50324. The tests were performed in a reciprocating motion mode with a “pin-on-disc” configuration. A ball made of WC–Co hard alloy (VK6) was used as the counterbody. The test conditions were as follows: linear speed – 10 cm/s, applied load – 2 N, track length – 4 mm, and total running distance – 10,000 cycles. The profiles of the wear tracks were studied using a WYKO NT 1100 optical profilometer (Veeco, USA).

## Results and discussion

After processing (mixing) in the planetary ball mill for 15, 30 and 45 min, the technological properties of each powder mixture were determined: flowability, bulk density, and particle size distribution. The results are presented in Table 2.

The obtained powder mixtures did not exhibit flowability when tested according to GOST 20899-98. Minor variations in bulk density values are associated with differences in particle sizes. The lack of flowability and low bulk density are due to the high dispersion of the powder mixture (average particle size 10–16 µm). Changes in particle size distribution are explained by the different milling durations: 15, 30 and 45 min. In the latter case, the particles tend to agglomerate. Further studies were conducted on the powder mixture processed in the planetary ball mill for 30 min,

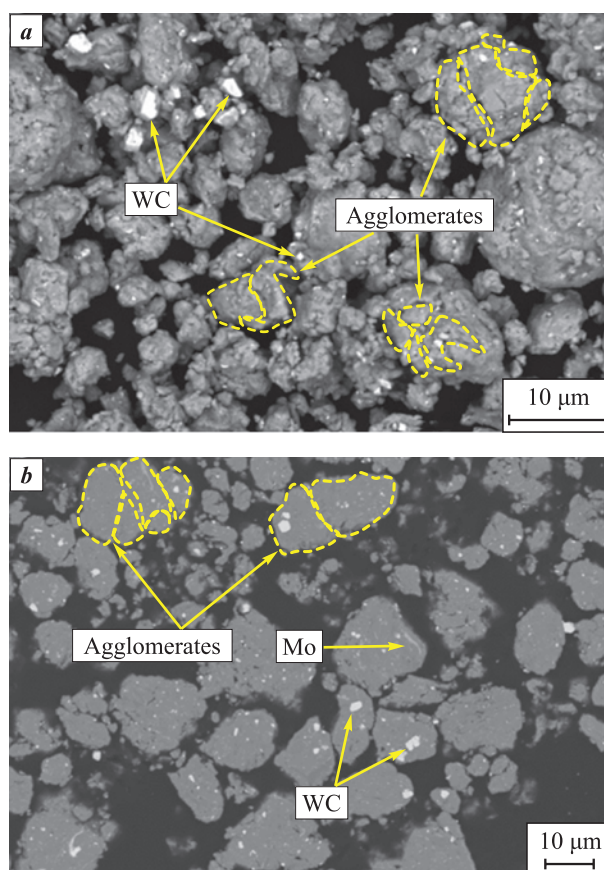


Fig. 1. SEM images of the morphology of HSS powder mixture particles (a) and their microstructure in cross-section (b)

Рис. 1. РЭМ-изображения морфологии частиц (a) порошковой смеси БРС и их микроструктуры на поперечном шлифе (b)

which is optimal for achieving a dispersed particle size distribution.

Figure 1 shows SEM images of the morphology of the powder mixture particles and their microstructure on a cross-section. It can be seen that the powder mixture particles range in size from 2 to 25 µm, with a near-spherical shape, and larger particles are agglomerates. The images were obtained in backscattered electron detection mode, which highlights heavy alloying elements (tungsten and molybdenum) by contrast,

Table 2. Technological properties of the HSS powder mixture at different processing durations of the PBM

Таблица 2. Технологические свойства порошковой смеси БРС при различной длительности обработки в ПЦМ

Processing duration, min	Flowability, s	Bulk density, g/cm <sup>3</sup>	Particle size distribution range, µm	Average particle size, µm	Distribution quantile $D_{50}$ , µm
15	Does not flow	2.66	6–30	12	11
30		2.50	3–30	10	8
45		2.90	4–30	16	12



distributed both on the surfaces and within the iron particles.

The presence of the introduced ceramic is detected only through general EDS analysis of the observed areas, indicating a high uniformity of the dispersion of the additive within the powder mixture, without the formation of separate agglomerates.

Figure 2 shows the dependence of the relative density of the billets on the compaction pressure after pressing and sintering. The dependencies show that during cold pressing, the powder mixtures are compacted to achieve a relative density of up to 69.8 % at a pressure of 900 MPa. After sintering, the density increases to 92.7 %. The highest hardness ( $62.0 \pm 1.0$  HRA) is observed in the densest sintered billets, pressed at  $P = 900$  MPa. The high level of compressibility during cold pressing is provided by the iron-based matrix powder.

The significant increase in density during sintering indicates an intense process at  $1200^\circ\text{C}$ . This is due to the high initial dispersion of the powder mixture, which provides an increased specific surface area and promotes the activation of sintering. The presence of boron lowers the temperature of liquid phase formation in the steel, further activating the sintering process [10; 17]. This may result in the formation of some amount of liquid phase.

Figure 3 shows SEM images of the microstructure of the sintered sample of R6M5K5 steel with ceramic additive, pressed at  $P = 900$  MPa. The microstructure of the sintered billet is quite homogeneous and porous, with alloying elements not forming carbide compounds  $\text{Me}_6\text{C}$  and  $\text{MeC}$ , which ensure the red hardness of HSS. The effect of the ceramic additive on the microstructure images and EDS analysis results is difficult to assess. In

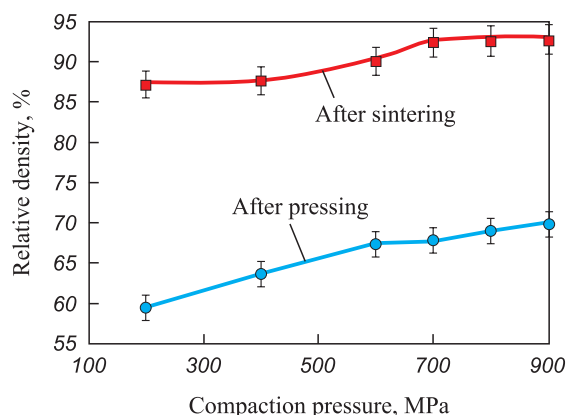


Fig. 2. Dependence of relative density of billets on compaction pressure before and after sintering

Рис. 2. Зависимость относительной плотности заготовок от давления прессования до и после спекания

Fig. 3, *b*, grains of the matrix with a size of  $3\text{--}8\ \mu\text{m}$  can be distinguished. The general elemental EDS analysis (integral area in Fig. 3, *a*) shows the presence of Hf and Si, which are part of the ceramic but not included in the composition of R6M5K5 steel itself (Table 3). This indicates significant dissolution of the ceramic additive in the steel matrix.

After hot pressing the powder mixture, the obtained billet had a hardness of  $64.0 \pm 0.3$  HRC with a relative density of 97.2 %, and after heat treatment, the hardness changed slightly to  $64.7 \pm 0.2$  HRC. The high hardness of the hot-pressed billet is due to the low temperature of hot pressing, which preserves a finer grain structure. During prolonged holding during annealing and austenitization at high temperatures, inevitable grain growth occurs. The increase in hardness after heat treatment is largely due to the formation of a carbide network during quenching and secondary carbides during tempering [19].

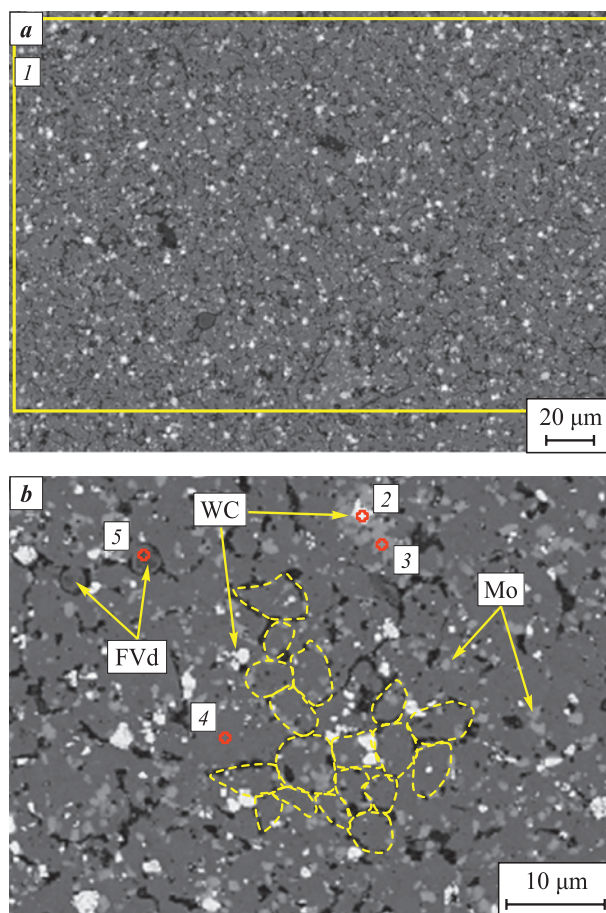


Fig. 3. SEM images of the microstructure of the sintered sample at  $500\times$  (*a*) and  $2000\times$  (*b*) magnification

Рис. 3. РЭМ-изображения микроструктуры спекшего образца при увеличении  $500\times$  (*a*) и  $2000\times$  (*b*)

**Table 3. Results of general and EDS analyses of microstructural components of the sintered HSS billet (see Fig. 3)**

**Таблица 3. Результаты общего и ЭДС анализов микроструктурных составляющих спеченной заготовки БРС (см. рис. 3)**

Area (component)	Content, at. %									
	C	V	Cr	Fe	Mo	Hf	W	Co	O	Si
1 (General)	20.4	2.4	3.8	58.4	4.0	0.4	1.8	2.5	3.7	2.7
2 (WC)	81.5	—	—	2.4	—	—	16.2	—	—	—
3 (Mo)	62.0	3.3	2.4	14.5	16.2	—	1.8	—	—	—
4 (Matrix)	17.2	0.4	2.4	78.6	1.2	—	0.3	—	—	—
5 (FVd)	27.1	37.3	2.4	25.4	2.9	—	4.8	—	—	—

Figure 4 shows SEM images of the microstructure of the hot-pressed billet after heat treatment. As seen from the data, carbide  $\text{Me}_6\text{C}$  with characteristic morphology is distributed along the grain boundaries, which is more typical for cast HSS [18; 20]. This may indicate the formation of a significant amount of liquid phase due to the melting of eutectic as a result of the influence of boron with the precipitation of eutectic carbide  $\text{Me}_6\text{C}$ , necessitating quenching at lower temperatures [17; 19]. In the matrix, represented by a solid solution based on iron, alloying elements are dissolved. After hot pressing followed by heat treatment, the introduced ceramic particles are fixed in the micro-

structure (marked in Fig. 4, *b* according to the presumed phases). The average grain size is 14–34  $\mu\text{m}$ , and the size of the ceramic particles is 2–4  $\mu\text{m}$ . Secondary carbide  $\text{MeC}$  is not detected, and vanadium, according to EDS results (Table 4), is contained in the matrix and  $\text{Me}_6\text{C}$  carbide. Secondary carbide  $\text{MeC}$  is not observed in the studied microstructure areas and XRD results (Table 5), as evidenced by the slight increase in hardness after heat treatment.

According to XRD data, the following phases are identified:  $\alpha\text{-Fe}$  (matrix), carbide  $\text{Me}_6\text{C}$  ( $\text{W}_3\text{Fe}_3\text{C}/\text{Mo}_3\text{Fe}_3\text{C}$ ), as well as  $\text{HfO}_2$  and  $\text{HfSiO}_4$ , which is consistent with

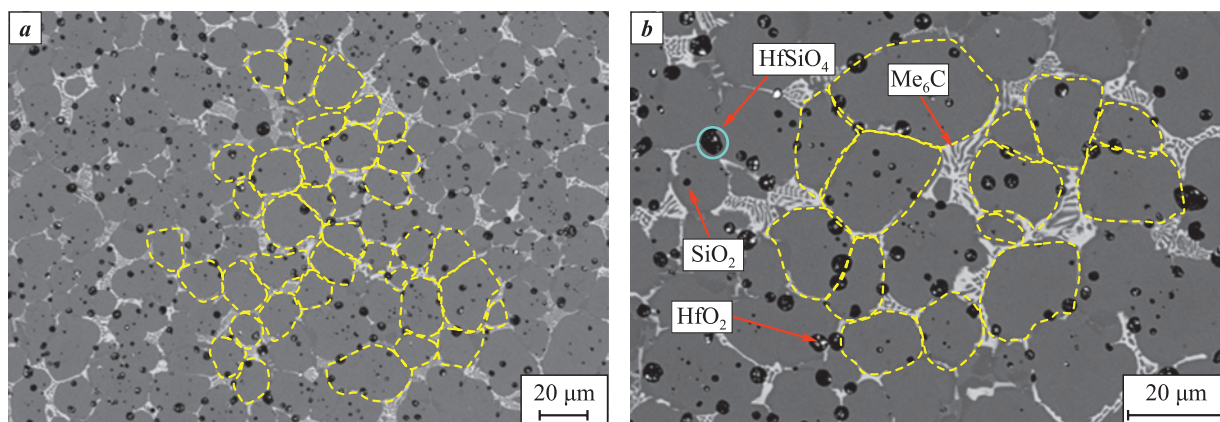


**Fig. 4. SEM images of the microstructure of the hot-pressed biller after heat treatment**

**Рис. 4. РЭМ-изображения микроструктуры горячепрессованной заготовки после термообработки**

**Table 4. Results of EDS analysis of microstructural components of the hot-pressed HSS billet**

**Таблица 4. Результаты ЭДС-анализа микроструктурных компонентов горячепрессованной заготовки БРС**

Component	Content, at. %										
	C	O	Si	V	Cr	Mn	Fe	Co	Mo	Hf	W
Matrix	14.3	—	—	1.4	3.7	—	74.5	2.8	2.1	—	1.3
$\text{HfSiO}_4$	9.8	60.2	20.0	0.9	—	0.4	2.6	0.1	0.4	5.6	—
$\text{HfO}_2$	18.5	57.9	—	—	0.5	—	3.6	0.4	1.3	17.7	—
$\text{SiO}_2$	11.2	61.3	20.6	1.3	0.6	0.2	4.3	—	0.5	—	—
$\text{Me}_6\text{C}$	31.9	—	—	4.8	3.9	—	32.8	1.6	15.6	—	9.4

**Table 5. XRD results of the hot-pressed R6M5K5 billet with ceramic additive****Таблица 5. Результаты РФА горячепрессованной заготовки Р6М5К5 с керамической добавкой**

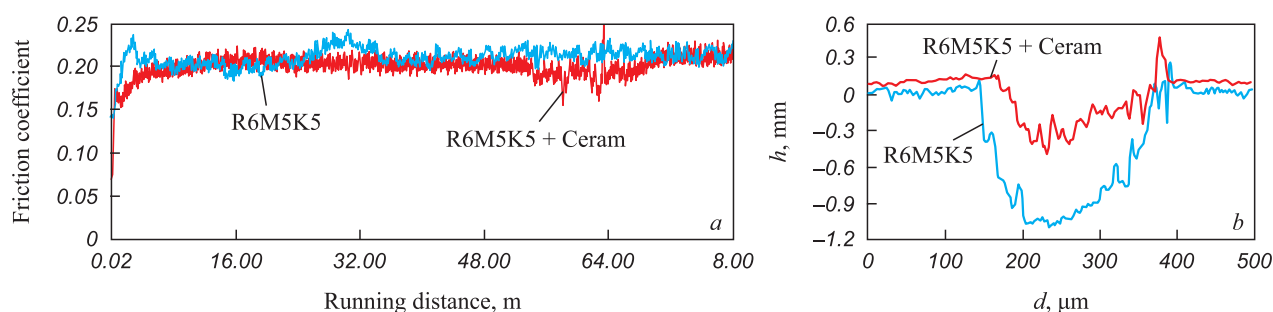
Phase	Structural type	Volume fraction, %	Lattice parameter, Å
$\alpha$ -Fe	<i>cI2/1</i>	82.4	$a = 2.890$
$\text{Me}_6\text{C}$	<i>cF112/2</i>	9.9	$a = 11.026$
$\text{HfSiO}_4$	<i>tI24/3</i>	1.6	–
$\text{HfO}_2$	<i>mP12/3</i>	1.5	–
Austenite	<i>cF4/1</i>	4.5	$a = 3.612$

the microstructure analysis results. Ceramic inclusions (Fig. 5) may represent hafnium silicate, which could form during the hot-pressing process or subsequent heat treatment [15; 21]. White particles in the structure of the ceramic additive (see Fig. 4, Table 4) in some areas are similar in composition to  $\text{HfO}_2$ , indicating incomplete interaction of  $\text{HfO}_2$  with  $\text{SiO}_2$ , which forms  $\text{HfSiO}_4$  [21]. Accordingly, the black areas are similar in composition to  $\text{SiO}_2$ .

The strength characteristics of the hot-pressed billets were studied: the bending and compressive strength values were  $1141 \pm 50$  and  $2157 \pm 42$  MPa, respectively. Additionally, the red hardness of the hot-pressed samples was determined by annealing in air for 4 h at 630 °C. The hardness after annealing was  $59.5 \pm 0.8$  HRC, meeting the requirements of GOST 19265-73.

Figure 5 shows the effect of the ceramic additive on the friction coefficient dependence on the running distance and the 2D profile of the wear track of hot-pressed powder high-speed steel R6M5K5 billets. It was found that they have a consistently low friction coefficient (0.20–0.22) when sliding against a VK6 alloy ball. The specific wear values calculated from the 2D profiles of the wear tracks were  $5.40 \cdot 10^{-6}$  and  $2.56 \cdot 10^{-6}$  mm<sup>3</sup>/(N·m) for the R6M5K5 and R6M5K5 + ceramic billets, respectively. Thus, the ceramic additive doubles the wear resistance of R6M5K5 steel (see Table 5). This is primarily due to the high hardness ( $64.0 \pm 0.3$  HRC) of the sample, owing to the formation of a carbide network and hard particles of  $\text{SiO}_2$  and  $\text{HfO}_2$ . However, the specific wear of the counterbody (Table 6) is twice as high when testing R6M5K5 with the ceramic additive.

According to [22], the increase in the actual contact area of the tribopair is accompanied by an increase in the friction coefficient. However, when sliding the ball on the R6M5K5 sample with the ceramic additive, this parameter did not change. The wear track of the R6M5K5 billet with the ceramic additive was studied using SEM (Fig. 6). At its edge, corresponding products in the form of flake-like agglomerates are present. According to EDS data (Table 7), they represent a mixture of oxidized counterbody and steel particles. Also, an adhered layer of oxidized wear products from the sample and counterbody was found in the wear track area. The pronounced heterogeneous

**Fig. 5. Dependence of friction coefficient on running distance (a) and 2D profiles of wear tracks (b) of hot-pressed R6M5K5 steel billets and R6M5K5 steel billets with ceramic additive**

**Рис. 5. Зависимость коэффициента трения от длины пробега (a) и изображение 2D-профилей дорожек износа (b) горячепрессованных заготовок из стали Р6М5К5 и Р6М5К5 + керамическая добавка**

**Table 6. Results of tribological tests****Таблица 6. Результаты трибологических испытаний**

Sample	Specific wear, $10^{-6}$ mm <sup>3</sup> /(N·m)		Friction coefficient		
	Sample	Counterbody	Initial	Average	Final
R6M5K5	5.40	0.20	0.41	0.22	0.23
R6M5K5 + ceramic	2.56	0.47	0.40	0.20	0.20



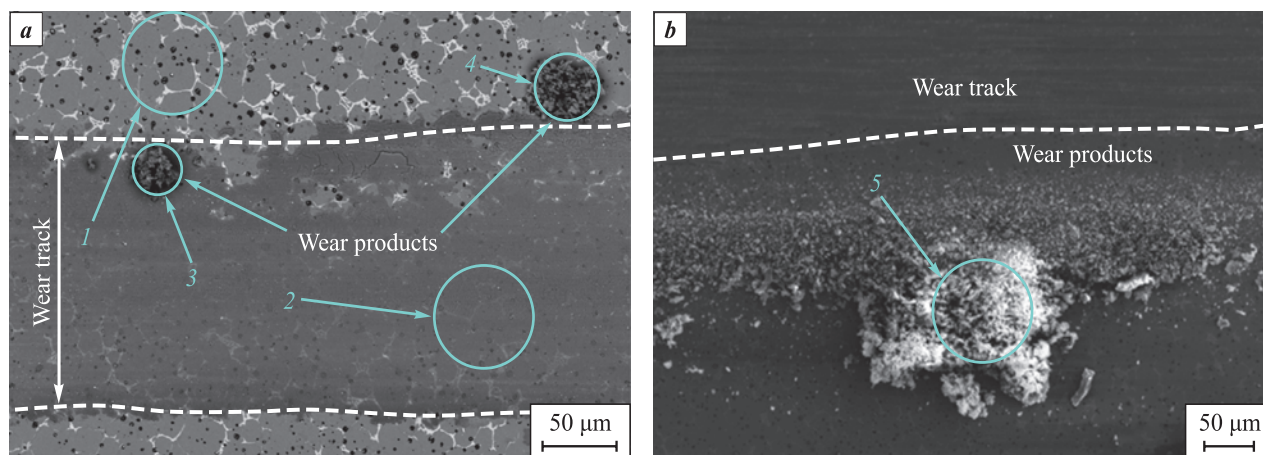


Fig. 6. SEM images of the wear track of the hot-pressed sample (a) and wear products (b)

Рис. 6. РЭМ-изображения дорожки износа горячепрессованного образца (a) и продуктов износа (b)

Table 7. Results of EDS analysis of wear track components

Таблица 7. Результаты ЭДС-анализа компонентов дорожки износа

Area No. in Fig. 6	Content, at. %									
	C	O	Si	V	Cr	Fe	Co	Mo	Hf	W
1	19.5	—	2.3	2.2	3.5	64.0	3.8	3.0	0.2	1.6
2	9.8	54.3	—	1.2	1.6	27.0	1.6	1.3	0.1	3.1
3	12.6	51.7	—	0.9	1.7	28.1	1.6	—	0.1	3.3
4	12.9	46.3	2.3	1.2	2.2	28.5	1.9	0.4	1.9	2.4
5	44.9	38.9	0.5	0.5	0.7	11.9	0.6	0.6	0.1	1.3

structure with ceramic inclusions is similar to the structure of powder metallic glass materials [23].

During wear,  $\text{HfO}_2$ ,  $\text{SiO}_2$  and  $\text{HfSiO}_4$  particles may contribute to its reduction [24]. The formed carbide structure is more preferable from the wear resistance perspective compared to dispersed carbides [25]. It can be assumed that the obtained composite material, demonstrating high red hardness, can also find application in the production of wear-resistant products operating at temperatures up to 630 °C.

## Conclusions

1. Sintered and hot-pressed billets of HSS grade R6M5K5 with a 3 % addition of heterophase ceramic  $\text{MoSi}_2\text{--MoB--HfB}_2$  were obtained, achieving relative densities of up to 92.7 % and 97.2 %, respectively. The hardness of the sintered billet was 62.0 HRA, while the hot-pressed billet reached 64.7 HRC. Both billets exhibited a bending strength of 1141 MPa and a compressive strength of 2157 MPa.

2. It was established that the hot-pressed billet is characterized by a pronounced heterogeneous microstructure, similar to that of metallic glass materials.

3. Tribological tests showed that the addition of the ceramic  $\text{MoSi}_2\text{--MoB--HfB}_2$  to the hot-pressed R6M5K5 high-speed steel billet resulted in more than a twofold increase in wear resistance.

4. A method for further improvement of the physical and mechanical properties is proposed by introducing a smaller amount of boron-containing ceramic additive and performing quenching at lower temperatures.

## References / Список литературы

1. Kostikov V.I., Ereemeeva Zh.V. Technology of composite materials: Textbook. Moscow: Vologda: Infra-Inzheneriya, 2021. 484 p. (In Russ.).  
Костиков В.И., Еремеева Ж.В. Технология композиционных материалов: Учебное пособие. М.: Вологда: Инфра-Инженерия, 2021. 484 с.
2. Matula G., Dobrzański L.A., Herranz G., Várez A., Levenfeld B., Torralba J.M. Structure and properties of HS6-5-2 type HSS manufactured by different P/M methods. *Journal of Achievements in Materials and Manufacturing Engineering*. 2007;24:71–74.
3. Liu Z.Y., Khor K.A., Tor S.B. Mechanical alloying of TiC/M2 high speed steel composite powders and sintering investigation. *Materials Science and Engineering: A*. 2001;



- 311:31–21.  
[https://doi.org/10.1016/S0921-5093\(01\)00929-7](https://doi.org/10.1016/S0921-5093(01)00929-7)
4. Herranz G., Matul G., Alonso R., Sánchez I., Rogriguez G. Metal injection moulding of carbides reinforced M2 HSS. *Proceedings of the Euro International Powder Metallurgy Congress and Exhibition*. 2009;2:99–104.
5. Herranz G., Romero A., de Castro V., Rodríguez G.P. Processing of AISI M2 high speed steel reinforced with vanadium carbide by solar sintering. *Materials & Design*. 2014;54:934–946.  
<https://doi.org/10.1016/j.matdes.2013.09.027>
6. Hadian A., Gorjan L., Clemens F.J. Thermoplastic processing and debinding behavior of NbC-M2 high speed steel cemented carbide. *Journal of Materials Processing Technology*. 2019;263:91–100.  
<https://doi.org/10.1016/j.jmatprotec.2018.08.006>
7. Madej M. Phase reactions during sintering of M3/2 based composites with WC additions. *Archives of Metallurgy and Materials*. 2013;58(3):703–708.  
<https://doi.org/10.2478/amm-2013-0058>
8. Chen N., Luo R., Xiong H., Li Z. Dense M2 high speed steel containing core-shell MC carbonitrides using high-energy ball milled M2/VN composite powders. *Materials Science and Engineering: A*. 2020;771:138628.  
<https://doi.org/10.1016/j.msea.2019.138628>
9. Thavale V.T., Dhokey N.B. Wear behavior and machinability of hot pressed sintering of B4C reinforced M3/2 HSS composite. *Materials Today: Proceedings*. 2021;44(6):4891–4897.  
<https://doi.org/10.1016/j.matpr.2020.11.710>
10. Zhang F., Luo P., Ouyang Q., He Q., Hu M., Li S. microstructure and mechanical properties of B<sub>4</sub>C-blended M3:2 high-speed steel powders consolidated by sintering and heat treatment. *Journal of Materials Engineering and Performance*. 2019;28:6145–6156.  
<https://doi.org/10.1007/s11665-019-04347-x>
11. German R.M. Supersolidus liquid-phase sintering of pre-alloyed powders. *Metallurgical and Materials Transactions A*. 1997;28(7):1553–1567.  
<https://doi.org/10.1007/s11661-997-0217-0>
12. Lapshin O.V., Boldyreva E.V., Boldyrev V.V. Role of mixing and milling in mechanochemical synthesis (Review). *Russian Journal of Inorganic Chemistry*. 2021;66(3):433–453.  
<https://doi.org/10.1134/S0036023621030116>  
Лапшин О.В., Болдырева Е.В., Болдырев В.В. Роль смешения и диспергирования в механохимическом синтезе (обзор). *Журнал неорганической химии*. 2021;66(3):402–424. <https://doi.org/10.31857/S0044457X21030119>
13. Avvakumov E.G. Mechanical methods for activating chemical processes. 3<sup>rd</sup> ed. Moscow: LENAND, 2022. 306 p. (In Russ.).  
Аввакумов Е.Г. Механические методы активации химических процессов. Изд. 3-е. М.: ЛЕНАНД, 2022. 306 с.
14. Antsiferov V.N., Antsiferova I.V. Features of sintering using nanosized carbide powders (scientific review). *Vestnik PNPU. Mashinostroyeniye, materialovedeniye*. 2015;2:66–76. (In Russ.).  
Анциферов В.Н., Анциферова И.В. Особенности процессов спекания с использованием наноразмерных твердосплавных порошков (научный обзор). *Вестник ПНИПУ. Машиностроение, материаловедение*. 2015;2:66–76.
15. Potanin A.Yu., Vorotilo S., Pogozhev Yu.S., Rupasov S.I., Lobova T.A., Levashov E.A. Influence of mechanical activation of reactive mixtures on the microstructure and properties of SHS-ceramics MoSi<sub>2</sub>–HfB<sub>2</sub>–MoB. *Ceramics International*. 2019;45(16):20354–20361.  
<https://doi.org/10.1016/j.ceramint.2019.07.009>
16. Potanin A.Yu., Pogozhev Yu.S., Levashov E.A., Novikov A.V., Shvindina N.V., Sviridova T.A. Kinetics and oxidation mechanism of MoSi<sub>2</sub>–MoB ceramics in the 600–1200°C temperature range. *Ceramics International*. 2017;43(13):10478–10486.  
<https://doi.org/10.1016/j.ceramint.2017.05.093>
17. Bendereva E.D., Vylkanov S.T. Activating effect of boron microadditions on sintering of powder alloy based on iron. *Metallurgist*. 2012;55(9-10):761–768.  
<https://doi.org/10.1007/s11015-012-9500-4>
18. Geller Ju.A. Tool steels. 4<sup>th</sup> ed. Moscow: Metallurgiya, 1975. 584 p. (In Russ.).  
Геллер Ю.А. Инструментальные стали. Изд. 4-е. М.: Металлургия, 1975. 584 с.
19. Chaus A.S. Structural and phase changes in carbides of the high-speed steel upon heat treatment. *The Physics of Metals and Metallography*. 2016;117:684–692.  
<https://doi.org/10.1134/S0031918X16070048>
20. Ha T. K., Yang E. I., Jung J. Y., Park S. W. Effect of alloying elements and homogenization treatment on carbide formation behavior in M2 high-speed steels. *Korean Journal of Metals and Materials*. 2010;48(7):589–597.  
<https://doi.org/10.3365/KJMM.2010.48.07.589>
21. Potanin A.Yu., Vorotilo S., Pogozhev Yu.S., Rupasov S.I., Loginov P.A., Shvyndina N.V., Sviridova T.A., Levashov E.A. High-temperature oxidation and plasma torch testing of MoSi<sub>2</sub>–HfB<sub>2</sub>–MoB ceramics with single-level and two-level structure. *Corrosion Science*. 2019;158:108074.  
<https://doi.org/10.1016/j.corsci.2019.07.001>
22. Kragel'skiy I.V. Friction and wear. 2<sup>nd</sup> ed. revised and updated. Moscow: Mashinostroyeniye, 1968. 480 p. (In Russ.).  
Крагельский И.В. Трение и износ. Изд. 2-е перераб. и доп. М.: Машиностроение, 1968. 480 с.
23. Libenson G.A. Production of powder products: Textbook for technical schools. 2<sup>nd</sup> ed. revised and updated. Moscow: Metallurgiya, 1990. 240 p. (In Russ.).  
Либенсон Г.А. Производство порошковых изделий: Учебник для техникумов. 2-е изд., перераб. и доп. М.: Металлургия, 1990. 240 с.
24. Pereira N.F., Rubio C.J., dos Santos J.A., Houmard M., Câmara M., Rodrigues A. Drilling of nodular cast iron with a novel SiO<sub>2</sub> coating deposited by sol-gel process in HSS drill. *The International Journal of Advanced Manufacturing Technology*. 2019;105:1–13.  
<https://doi.org/10.1007/s00170-019-04429-z>
25. Chaus A.S., Hudáková M. Wear resistance of high-speed steels and cutting performance of tool related to structural factors. *Wear*. 2009;267(5-8):1051–1055.  
<https://doi.org/10.1016/j.wear.2008.12.101>

## Information about the Authors



**Amankeldy S. Akhmetov** – Scientific Project Engineer, Department of Powder Metallurgy and Functional Coatings (PM&FC), National University of Science and Technology “MISIS” (NUST MISIS)

 **ORCID:** 0000-0002-1606-838X

 **E-mail:** aman1aotero@gmail.com

**Samat K. Mukanov** – Cand. Sci. (Eng.), Junior Research Scientist, Laboratory “*In situ* Diagnostics of Structural Transformations”, Scientific Educational Center of Self-Propagating High-Temperature Synthesis, MISIS-ISMAN

 **ORCID:** 0000-0001-6719-6237

 **E-mail:** sam-mukanov@mail.ru

**Vladimir Yu. Lopatin** – Cand. Sci. (Eng.), Associate Professor, Department of PM&FC, NUST MISIS

 **ORCID:** 0000-0002-1294-9198


 **E-mail:** lopatin63@mail.ru

**Marina E. Samoshina** – Cand. Sci. (Eng.), Head of the Division of Academic Degrees, Academic Secretary of the Dissertation Board, NUST MISIS

 **ORCID:** 0009-0000-2773-3122

 **E-mail:** samoshina@list.ru

**Zhanna V. Ereemeeva** – Dr. Sci. (Eng.), Professor, Department of PM&FC, NUST MISIS

 **ORCID:** 0000-0002-1790-5004

 **E-mail:** ereemeeva-shanna@yandex.ru

## Сведения об авторах

**Аманкельды Серикбаевич Ахметов** – инженер научного проекта, кафедра порошковой металлургии и функциональных покрытий (ПМиФП), Национальный исследовательский технологический университет «МИСИС» (НИТУ МИСИС)

 **ORCID:** 0000-0002-1606-838X

 **E-mail:** aman1aotero@gmail.com

**Самат Куандыкович Муканов** – к.т.н., мл. науч. сотрудник лаборатории «*In situ* диагностика структурных превращений» Научно-учебного центра СВС, МИСИС-ИСМАН

 **ORCID:** 0000-0001-6719-6237

 **E-mail:** sam-mukanov@mail.ru


**Владимир Юрьевич Лопатин** – к.т.н., доцент кафедры ПМиФП, НИТУ МИСИС

 **ORCID:** 0000-0002-1294-9198

 **E-mail:** lopatin63@mail.ru

**Марина Евгеньевна Самошина** – к.т.н., начальник отдела учебных степеней, ученый секретарь диссертационного совета, НИТУ МИСИС

 **ORCID:** 0009-0000-2773-3122

 **E-mail:** samoshina@list.ru

**Жанна Владимировна Еремеева** – д.т.н., профессор кафедры ПМиФП, НИТУ МИСИС

 **ORCID:** 0000-0002-1790-5004

 **E-mail:** ereemeeva-shanna@yandex.ru

## Contribution of the Authors



**A. S. Akhmetov** – conducted experiments, prepared the manuscript of the article.

**S. K. Mukanov** – participated in editing the text of the article, studied the features of tribological tests, and discussed the results.

**M. E. Samoshina** – participated in editing the text of the article, participated in the discussion of the results.

**V. Yu. Lopatin** – participated in the discussion of the results.

**Zh. V. Ereemeeva** – conceptualization of the study, participated in the discussion of the results.

## Вклад авторов

**А. С. Ахметов** – проведение экспериментов, подготовка текста статьи.

**С. К. Муканов** – исследование особенностей трибологических испытаний, участие в обсуждении результатов, подготовка текста статьи.

**М. Е. Самошина** – участие в обсуждении результатов, корректировка текста статьи.

**В. Ю. Лопатин** – участие в обсуждении результатов.

**Ж. В. Еремеева** – концептуализация исследования, участие в обсуждении результатов.

Received 26.12.2023

Revised 18.03.2024

Accepted 21.03.2024

Статья поступила 26.12.2023 г.

Доработана 18.03.2024 г.

Принята к публикации 21.03.2024 г.